Vehicular Communications 34 (2022) 100424

Contents lists available at ScienceDirect

Vehicular Communications

www.elsevier.com/locate/vehcom

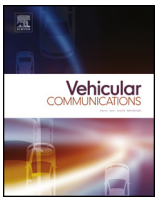

Beam management for vehicle-to-vehicle (V2V) communications in millimeter wave 5G

Luca Montero [a,*], Christian Ballesteros [a], Cesar de Marco [b], Luis Jofre [a]

[a] Universitat Politècnica de Catalunya (UPC), Jordi Girona 31, Barcelona, 08034, Spain
[b] SEAT S.A., A-2. Km. 585, Martorell, 08635, Spain

ARTICLE INFO

Article history:
Received 30 July 2021
Received in revised form 23 September 2021
Accepted 9 October 2021
Available online 14 October 2021

Keywords:
V2X
V2V
Beamforming
Beam management
5G
mmWave

ABSTRACT

Cooperative, Connected and Automated Mobility (CCAM) is expected to leverage the full potential of wireless communications. With the growing adoption of 5G and its support for Vehicle-to-Everything (V2X) communications, beamformed vehicular communications at millimeter-wave (mmWave) bands are expected to enable the most demanding connected driving applications. Beamformed V2X links present the challenge of beam management in such a fast-changing scenario. This paper goes through the practical limitations of the 5G V2X stack to support successful beamforming procedures. Two beam management strategies are proposed. Both strategies are evaluated in terms of power performance, beam recovery time and channel usage. The results suggest that significant differences apply when the beam is more frequently updated, whereas little improvement is seen by increasing the size of the beamset. Also, the selection of a proper strategy is shown to be important to alleviate the channel from overheads, and substantial differences in required signaling can be seen depending on the beam-tracking approach.

© 2021 The Author(s). Published by Elsevier Inc. This is an open access article under the CC BY-NC-ND license (http://creativecommons.org/licenses/by-nc-nd/4.0/).

1. Introduction

The automotive industry has recently emerged as one of the key vertical industries expected to extract the full potential of modern wireless communications. The foreseen transformation of mobility towards safer, more efficient transportation and the much-anticipated inclusion of increasingly automated driving systems have accelerated the development of communication standards especially designed for vehicular communications. As such, vehicle-to-everything (V2X) has lately surfaced as the driving force to support a wide set of advanced driving applications that not only address the main concerns associated with the industry, but also constitute a roadmap for the envisioned Cooperative, Connected and Automated Mobility (CCAM) future.

Initial V2X implementations aimed at providing status information for driver awareness, and standards such as IEEE 802.11p and LTE-V2X offer sufficient performance to fulfill this goal. However, the next step in the CCAM roadmap goes through the integration of V2X data into the vehicle's decision-making to provide fail-safe automation. The 5th generation of mobile communications (5G) stands as a promising enabler for this objective, and the 3rd Generation Partnership Project (3GPP) recently gave support for a new set of applications by updating its V2X stack with New Radio (NR) features.

Applications such as cooperative perception and cooperative maneuvering will turn essential to increase the Levels of Automation (LoA), V2X will then serve both as a sensor beyond line of sight and a trustworthy negotiator, and hence reliability and quality of service (QoS) assurance will become paramount. With this forecast, V2X will need to leverage the full capacity of 5G, and this includes the use of the millimeter-wave (mmWave) band and the large available bandwidth it offers.

Operating at the mmWave band generally implies the use of beamforming techniques to focus the radiated power towards the intended transmitter or receiver, as propagation at these frequencies suffer from increased attenuation sources. Radiation in this situation is not omnidirectional, but based on sharp beams where power is concentrated in a specific angular region in space. Therefore, communicating pairs need to maintain their beams constantly aligned to prevent outage and additional signaling between them is required for this purpose. Beamforming to communicate with a static base station is now possible and the mechanisms are widely present in the specifications [1], but the same does not apply for beam-based device-to-device (D2D) – e.g., vehicle-to-vehicle (V2V) – links, which still remain an open research topic.

The need for sidelink (SL) beamforming was recently introduced in 3GPP discussions [2], where beam-based operation is suggested to be supported for all bands to reduce interference in V2X scenar-

* Corresponding author.
E-mail address: luca.montero@upc.edu (L. Montero).

https://doi.org/10.1016/j.vehcom.2021.100424
2214-2096/© 2021 The Author(s). Published by Elsevier Inc. This is an open access article under the CC BY-NC-ND license (http://creativecommons.org/licenses/by-nc-nd/4.0/).

ios. In [3], the benefits of beamformed vehicular communications on interference are analyzed and promising results on resource reuse are presented.

Beam management, conceived as the set of procedures to acquire and update the optimum beams for communications, is gaining importance in V2X studies. In [2], the specification of beam management procedures for SL is proposed, suggesting the use of NR mechanisms as the baseline. A deeper look into how these mechanisms could be adapted for vehicular communications is then detailed in [1]. Nevertheless, the developments found in the literature tend to idealize channel and antenna modeling; as in [4], where both channel and antenna set-ups are idealized to optimize the beamwidth of beamformed V2V links. In this paper, the performance of two beam management strategies for V2V is evaluated in practical channel realizations and antenna implementations, with the goal to obtain realistic representations of the behavior of beamforming in vehicular scenarios when the variability in vehicles' distributions and the channel among them is decisive for proper beam-based operation. To do so, the proposed strategies are defined so that they comply with the mechanisms expected to be used for such links, and thus, further realism is pursued by constraining the configurations to the signaling that they would require. In Section 2, the resources provided by 3GPP for beam management for NR is presented. In Section 3, the challenges and potential mechanisms to enable beamforming in V2X scenarios is described. Then, in Section 4, the simulation framework and the proposed strategies are detailed. Finally, the results of the performance of the strategies are comprehensively commented in Section 5.

2. Beam management in 5G NR

5G NR introduced in Release 14 support for analog beamforming at both the base station and the user equipment (UE) with the so-called beam management procedures. Forecasting the need for sharp steerable beams, pertinent to maintain links operating at the mmWave band, beam management comprises a set of features to align the beams at both ends and ensure link stability. The procedures include the following aspects:

- Beam determination: selection of a suitable beam at one or both ends of the link.
- Beam measurement: allowing both ends to measure the characteristics of the received beamformed signals.
- Beam reporting: whereby beam measurement information is fed back to the transmitter.
- Beam sweeping: covering an angular sector by switching to different analog beams over the area.

These features allow acquiring enough information to determine proper beam pairs (i.e., aligned transmitting and receiving beams) along a data session with low-layer signaling.

2.1. Procedures for beam management

Even though the 3GPP does not state unambiguously the specific method to perform beam management, the following procedures – described in [5] – are supported:

- P-1: specially used to find initial beam pairs, a beam sweep at the transmitter is performed to select one or more transmitting and (if possible) receiving beams.
- P-2: once a beam pair is determined, a smaller set of beams from the transmitter can be swept over a reduced angular region to maintain the link. If needed, this smaller set can consist of narrower beams – a process also known as beam refinement.
- P-3: focused on beam determination at the receiver side, a previously-determined transmitting beam is fixed during a receiver beam sweep.

Note that in each of the procedures, one or more suitable beam measurements can be reported to increase robustness against beam failure, thereby a fast recovery can be triggered upon blockage, misalignment or outage. Nevertheless, some of these procedures are meant to be done periodically, while others (such as beam refinement) can be triggered if conditions allow it. It is therefore worth considering the overheads produced by the required signaling, and aim for a trade-off between perfect, sharp beam alignment and coarse beam pairing to alleviate channel congestion.

2.2. Signals for beam measurement and reporting

The support of NR for mmWave frequencies and beamforming entails defining reference signals that allow beam management procedures.

2.2.1. Synchronization signals

To perform initial access and synchronization between UE and Base Station (BS), NR makes use of the Synchronization Signal (SS) Block, or SSB. Initially conceived for downlink (DL), an SSB spans 4 Orthogonal Frequency-Division Multiplexing (OFDM) symbols in time and 240 subcarriers in frequency. It comprises the Primary Synchronization Signal (PSS), the Secondary Synchronization Signal (SSS), as well as the Physical Broadcast Channel (PBCH) and its associated DeModulation Reference Signal (DMRS) [6].

In order to suit for beam management SSBs can be beamformed, and therefore, the 3GPP defines the so-called SS bursts, where a number of SSBs (N_{SSB}) can be transmitted to measure different beam pair combinations. Currently, the specifications support up to $N_{SSB} = 64$ per burst for mmWave bands, which are grouped in the first 5 ms (half frame) of the SS burst periodicity (T_{SS}). This potentially allows encapsulating 64 different beam measurements in 5 ms, in a process that can be periodically repeated every $T_{SS} = \{5, 10, 20, 40, 80, 160\}$ ms [7].

2.2.2. Channel state information

The Channel State Information (CSI) framework in NR is a complex scheme by which UEs can perform channel measurements and report relevant information for link configuration. In DL, base stations send UE-specific CSI Reference Signal (CSI-RS) with a high level of flexibility regarding its resource mapping, number of ports, and periodicity, and thus CSI-RS can be allocated virtually anywhere within the resource pool. Upon reception, the receiver measures the signals to issue a CSI report.

CSI-RS can also be beamformed to different angular regions providing a complementary, yet more flexible mechanism for beam management operations. As a result, CSI-RS can be used to perform additional beam searches during the remaining time between SS bursts. CSI-RS resources can be linked to the previous SSB, which can be convenient to update coarse beams in a surrounding reduced angular space, to trigger beam refinement, or even perform another full beam sweep in between. As such, CSI is indeed responsible of reporting which beamformed SSBs and CSI-RS resources have resulted in better received power in the measurements.

3. Beam management for V2X scenarios

Although NR V2X allegedly supports the same frame structure and spectrum options as those established for downlink/uplink

communications, the procedure to manage beamformed links in SL remains unspecified. This study aims to elucidate some of the main limitations that SL will experience for beam management aspects and also evaluate suitable strategies and configurations based on these constraints.

3.1. Challenges for beamformed V2V links

One concern that was raised with Long Term Evolution (LTE)-based V2X was the quick loss in reliability when tens of vehicles where simultaneously sharing the 10 MHz channel reserved for intelligent transportation systems (ITS) at 5.9 GHz. To increase resilience against interference, a need for additional bands for V2X was expressed by several studies in the field [8]. At the same time, the use cases defined for future V2X easily made LTE V2X and the 5.9 GHz ITS band to fall short at fulfilling the requirements imposed by the industry. As a result, it is agreed that NR V2X should support both licensed and unlicensed ITS bands for SL operation. Access to any band can be orchestrated by base stations in a time division fashion, except when nodes are out-of-coverage and have to schedule autonomously their transmissions. This latter case has been particularly relevant in the design of LTE V2X at 5.9 GHz, but with the introduction of NR V2X this scheduling can extend to new bands. In this line, mmWave bands such as the 30 GHz and 63 GHz bands have been object of study by 3GPP [9] as they provide enough bandwidth to support some of the most demanding use cases.

Beamforming has been established as one the key enablers to make use of these higher frequency bands. This increase in gain comes from focusing the power towards a specific angular range at the expense of less exerted power towards the remaining angles. Beamformed V2V links differ from V2I/V2N links in the sense that the pointing vectors between nodes are essentially spread over a 2D space – i.e. in the azimuth plane. This geometry has proved detrimental in sub-6 GHz bands, as interference between neighboring nodes became unwieldy with high vehicle densities; but using V2V beamforming at high frequencies might potentially reduce the interference radiated over unwanted directions which can be specially advantageous to alleviate channel congestion and enjoy better link performance [10,11].

The spatially filtered footprint generated by beamformed V2V links can also lead to a greater time-frequency resource re-use. The authors from [12] by addressing V2V resource association as a matching game problem yielded a 50% increase in the number of established V2V links compared to the minimum-distance and asynchronous long-term pairing approaches presented in [13]. Nevertheless, devising an optimum link distribution and resource allocation to maximize resource re-use is not a trivial exercise, as it would require extensive knowledge of node pair locations and their resource use expectations. An omniscient base station can support this scenario. However, out-of-coverage nodes will require autonomous resource selection and, as pointed in [14], even new hidden node scenarios can arise. As such, resource management for beamformed V2V links remains an open research challenge.

Another challenge for beamformed V2X links is beam management. Initial beam establishment and continuous tracking is often associated with overheads, which in the V2V case can easily congest the channel if complete, frequent beamsweeps are executed by all nodes. Solutions to this have been subject of study in the literature. Some approaches suggest using location data of the intended transmitter/receiver for beam determination, either by means of sensors [15,16] or periodic V2X messaging through the ITS band [14,15]. Also in [17], the authors suggest multiplexing data transmissions with beam trainings, which does not necessarily lead to overhead reduction, but can help reduce the latency associated with training.

The authors in [18] have tackled the beam update requirements for these scenarios by looking at the coherence time. When migrating from the ITS band at sub-6 GHz to the mmWave candidates, the Doppler spread can increase tenfold. As such, the inversely proportional channel coherence time can require too frequent channel measurements. Although the results from [19] show how using narrower beams can lead to more relaxed channel coherence times; it is suggested in [18] to use the beam coherence time as the baseline for realignment. The benefits in overheads when the beam update rate approaches the beam coherence time, representing the time over which the beams stay aligned – i.e. between the peak power and a defined loss ratio – appears to outweigh the loss due to channel time variation and suboptimal beam selection due to fading.

3.1.1. Considerations on V2X resources

The frame structure in NR V2X SL follows the same principles of NR. Resources are divided in Physical Resource Blocks (PRBs), which consist of 12 subcarriers in frequency and a slot (14 OFDM symbols) in time. Numerologies determine the subcarrier spacing (SCS), which relates to the slot duration (T_{slot}) in an anti-proportional manner [6]. At mmWave, $SCS^{\mu} = \{60, 120\}$ kHz are supported, making each PRB to span $T^{\mu}_{\text{slot}} = \{0.25, 0.125\}$ ms, respectively.

Adopting the resource grid used in NR allows for flexible resource allocation. In SL, the building block for this grid is a subchannel, which is a slot-long cluster of $N^{\text{sch}}_{\text{PRB}} = \{10, 12, 15, 20, 25, 50, 75, 100\}$ PRBs. It is thus worth noting that subchannel bandwidth will depend on numerology, but following the aforementioned anti-proportionality, when fewer subchannels can be accomodated in the available bandwidth, more slots will fit within a frame (10 ms).

With this arrangement, nodes using autonomous resource selection sense the available subchannels during a sensing window and determine which subchannels are unavailable for transmission, either by measuring an unacceptable level of interference (over a dynamic threshold) or by decoding the SL Control Information (SCI) of incoming transmissions, in which future resource reservations by other UEs are indicated. Then, resource selection by the sensing UE depends on multiple factors, as NR V2X supports both periodic and aperiodic traffic, as well as the newly introduced feedback-assisted unicast and groupcast. Generally, this resource selection will eventually depend on the priority and Quality of Service (QoS) requirements of the packet to be delivered, and therefore each UE will modulate its resource selection based on service requirements and whether the Channel Occupation Rate (CR) exceeds a certain threshold for congestion control [20]. Note that beamforming drastically reduces the interference spread over unwanted directions, so a mmWave SL data transmission will inherently exert less pressure on channel congestion than its sub-6 GHz counterpart, fostering greater spatial re-use of the time-frequency resources.

3.2. SL signaling for beam management

As suggested in [2], beam management should be supported in NR V2X using NR mechanisms as baseline. As such, both Sidelink-SSB (S-SSB) and CSI-RS should be used for beam sweeping and CSI reports must provide the necessary feedback for beam alignment.

Synchronization in SL is structured to unify the resources occupied by SS bursts across all supported bands. As NR V2X might need to co-exist with LTE V2X at some bands, the 10 MHz channel bandwidth – relevant in LTE V2X – is to be supported, and thus 11 PRBs (132 subcarriers) is established as the frequency scope for all NR V2X S-SSB [21,22]. The slot structure of each S-SSB to accomodate Sidelink-PSS (S-PSS), Sidelink-SSS (S-SSS) and Physical

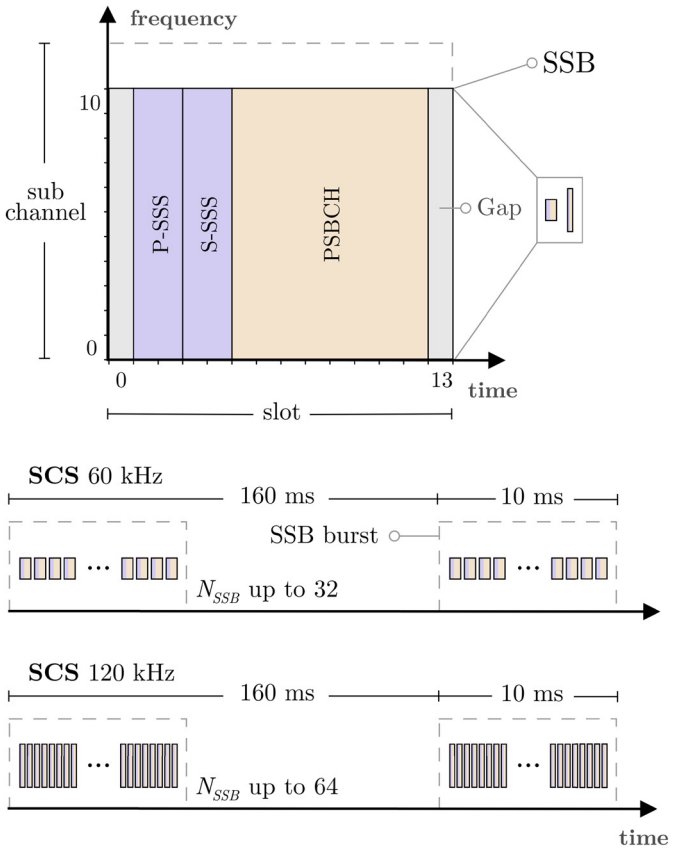

Fig. 1. SS Burst and S-SSB structure in NR V2X SL.

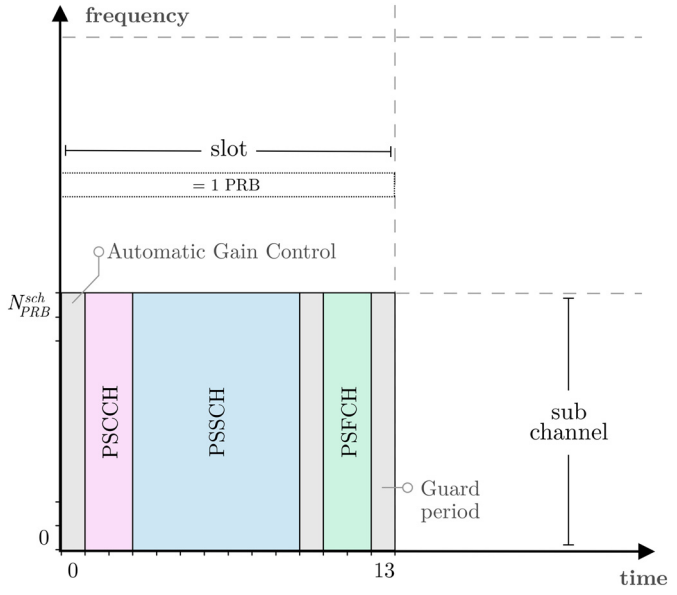

Fig. 2. Slot and resource grid structure in NR V2X SL [25].

Sidelink Broadcast Channel (PSBCH) [6] is depicted in Fig. 1. Using this structure, it is specified that up to $N_{SSB} = 64$ for 120 kHz SCS (up to 32 for 60 kHz SCS) can be encapsulated within an SS burst in a 10 ms window [7,21]. Finally, as also shown in Fig. 1, consecutive SS bursts are transmitted with a periodicity that is fixed to $T_{SS} = 160$ ms in SL [23].

The SS burst periodicity limits the ability of performing SS-based beam sweeps to 160 ms. Although the configurability of this parameter is suggested to be supported [21], complementary beam determination and refinement can be realized by CSI-RS in SL. As illustrated in Fig. 2, the slot structure in NR V2X is designed to accomodate the Physical Sidelink Shared Channel (PSSCH), the Physical Sidelink Control Channel (PSCCH) and the Physical Sidelink Feedback Channel (PSFCH) in a single subchannel. While PSCCH and PSFCH are used for general control information, resource reservation, and Hybrid Automatic Repeat Request (HARQ) feedback control, and are not necessarily present in all the PRBs that form a subchannel [20]; CSI-RS signals and the corresponding CSI reports are always allocated in the PSSCH [24]. The CSI-RS only supports 1 or 2 antenna ports, and an average of one resource element per PRB [6], assuming CSI-RS will extend across each PRB within the subchannel [7]. CSI reports, here as well, will provide feedback to the transmitter to indicate those resources most suitable for optimum reception.

Table 1
Configuration of vehicular traffic modeling for the case scenarios under evaluation.

	Urban	Highway
Description	9 blocks of Manhattan Grid	Two-way highway
Lanes	2 in each direction	3 in each direction
Lane width	3.5 m	4 m
Grid size	433 x 250 m	N/A
Simulation area	1299 x 750 m	2000 m
Vehicle velocity	60 km/h	80/100/140/40/30/20 km/h
Intersection turn probability	Going straight: 50% Turning left: 25% Turning right: 25%	N/A

4. Evaluation of SL beam management

4.1. Simulation framework

In order to evaluate beam management in realistic driving scenarios, the framework for simulation is designed so that the link performance between vehicles and the underlying channel realizations are calculated from a dataset that exemplifies a variety of microscopic traffic situations. Besides, to give flexibility to assess different beam management strategies, the measurements are based on parameterized antenna front-ends which can be preconfigured with standard-compliant beam steers.

4.1.1. Vehicular scenarios

Two traffic scenarios are modeled for the evaluation, Manhattan (urban) and highway, according to the evaluation methodologies of 3GPP for V2X [26]. The properties of each scenario are summarized in Table 1. To obtain realistic vehicle distributions across the scenarios, vehicles are dropped in Simulation of Urban Mobility (SUMO) tool [27] so that the distance between new vehicles in the same lane corresponds to a safety distance proportional to the lane speed. Vehicle dropping thus follows an exponential probability distribution where the mean time gap between consecutively dropped vehicles is 2 s at the lane speed. In the simulation, dropped vehicles interact with each other following basic traffic rules.

4.1.2. Antenna configuration

Vehicles in the simulation carry a mmWave antenna system with four antenna panels operating in the n257 5G band (26.50 – 29.50 GHz). Each panel sectorizes the azimuth plane in a way that each one faces its corresponding 90° sector – for convenience: the front, back and sides of the vehicle. The panels consist of multi-element antenna arrays with beamforming capabilities designed to cover the steering range required for each sector (±45°).

As V2V links occur in the same elevation plane, the antenna arrays in this calculation have a single vertical element, whereas the required steering range in azimuth is covered with N_{ant} horizontally arranged elements. Each panel operates with a pre-configured beamset with N_{c} coarse beams and N_{f} fine beams. The fine beams are formed with a generalized Discrete Fourier Transform (DFT) codebook with an offset of $-(1+N_{\text{ant}})/2$. The weights for analog beamforming for each of these beams ($\mathbf{u}_i$) is expressed as in [28]:

$$\mathbf{u}_i = \frac{1}{\sqrt{N_{\text{ant}}}}\left[e^{-j\frac{2\pi}{N_{\text{f}}}\left(i-\frac{N_{\text{f}}+1}{2}\right)}, e^{-j\frac{2\pi}{N_{\text{f}}}2\left(i-\frac{N_{\text{f}}+1}{2}\right)}, \ldots, e^{-j\frac{2\pi}{N_{\text{f}}}N_{\text{ant}}\left(i-\frac{N_{\text{f}}+1}{2}\right)}\right], \tag{1}$$

where $i = 1, 2, \ldots, N_{\text{f}}$ and, depending on the oversampling (O) of the codebook, the number of fine beams is $N_{\text{f}} = O N_{\text{ant}} + 1$. This method quantizes the angular space and uniformly covers the steering range. Coarse beams are then formed by combining fine beams in a hierarchical fashion. By assuming a fully-connected hybrid beamforming architecture with N_{RF} RF ports, N_{RF} beams can potentially be combined to create increasingly wide beams. The antenna system thus combines fine beams into coarser widths using:

$$\mathbf{v}_k = \frac{1}{\sqrt{N_{\text{RF}}}}\sum \mathbf{u}_p\, e^{jw_{\text{o}}p}, \tag{2}$$

where $k = 1, 2, \ldots, N_{\text{c}}$. Here, p denotes the indices of each of the contiguous fine beams being combined. The parameter w_{o} is optimized for each different N_{RF} value so that the gain ripple of the aggregated radiation pattern is minimized.

4.2. Channel estimation

The channel modeling is performed for the vehicular scenarios detailed in Table 1. The link-level interactions are calculated by means of the Quasi Deterministic Radio Channel Generator (QuaDRiGa) tool [29] for the vehicle trajectories initially obtained in SUMO. The channel response is the result of geometry-based stochastic channel modeling (GBSCM) simulation based on the specifications of the 3GPP in [26]. GBSCM provides a trade-off between repeatability, generalization and accuracy. Purely stochastic models suffer from a lack of physical meaning and some spatial information is lost, whereas ray tracing tools offer a highly accurate channel model at the expense of very time consuming calculations. In addition, the latter reduces the applicability of the results to the specific scenario under study and it is constrained to the realism of the actual model.

Different visibility conditions between vehicles are considered following the abovementioned recommendations [26]: line of sight (LOS), non-line of sight (NLOS) (building blockage) and vehicle-blocked NLOS (NLOSv) (LOS path blocked by one or more vehicles). The QuaDRiGa channel calculations defines a set of arbitrary multipath radio channels by determining some initial settings with stochastic models, whereas the particular contributions of the scattering clusters are computed with the addition of various rays with individual angular and temporal features based on GBSCM [30].

4.3. Beam management strategies

In this study two beam management strategies constrained to the aforementioned tools provided by NR-V2X are compared to assess which one might be more suitable for V2V scenarios. A set of vehicle pairs in the scenario are linked and the strategies are evaluated by measuring the power received by each of the target nodes during the simulation time, being the results affected by visibility conditions and channel selectivity phenomena. The following strategies, and their underlying power profiles, are measured for the linked vehicle pairs under evaluation:

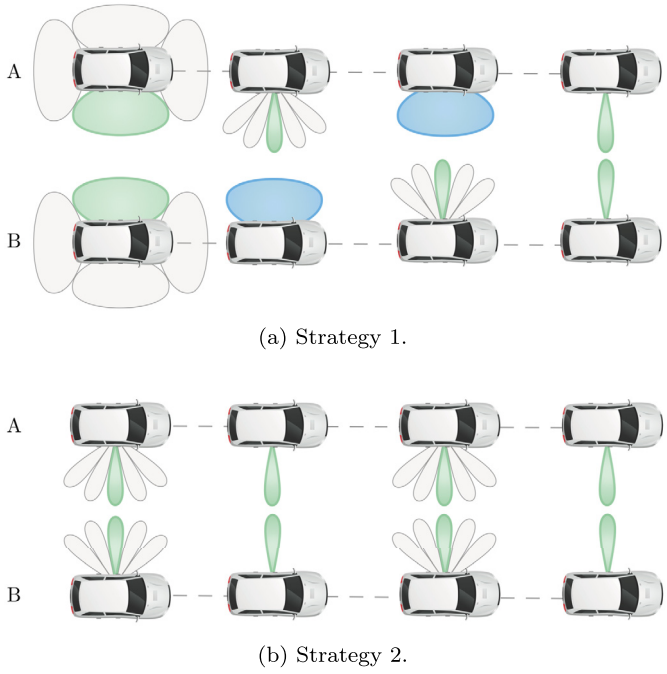

(a) Strategy 1.

(b) Strategy 2.

Fig. 3. Proposed beam management strategies for V2V beamforming.

- **Reference (R). Perfect beam-alignment**: all the fine beam combinations for both vehicles are measured every simulation snapshot and the beam pair that provides the maximum Reference Signal Receive Power (RSRP) is always chosen.
- **Strategy 1 (SG1). Coarse anchoring and refinement**: Every T_{SS} a SS burst measures all coarse beam combinations for both vehicles and defines a coarse anchor. Then, K_{CSI} CSI bursts are performed between SS bursts for each node, where a subset of $1 + N_{\text{ngh}}$ fine beams from the transmitter are measured using the coarse anchor from the receiver end, as shown in Fig. 3a. The transmitting fine beam that provides the maximum RSRP is chosen. The same process is also performed inversely K_{CSI} times to choose the most suitable receiving fine beam.
- **Strategy 2 (SG2). Fine tracking:** Both S-SSB and CSI are used to measure fine beams. Every T_{SS} and K_{CSI} times in between both nodes measure all combinations of a subset of $1 + N_{\text{ngh}}$ fine beams, as shown in Fig. 3b. The beam pair that provides the maximum RSRP is chosen until the next measurement. The initial beam is determined by a full sweep.

These two strategies exemplify two different approaches to tackle beam management in V2V scenarios. Both strategies aim to maintain a beamformed link with fine beams, yet present significant practical differences regarding stability, resource utilization and failure recovery. The reference signal is assumed as the maximum achievable power performance between the nodes. However, as it is unfeasible resource-wise to perform the reference measurement, the proposed strategies make use of (N_{ngh}) neighbor beams. When used, this subset of beams takes the previously chosen fine beam (from the previous measurement) and $N_{\text{ngh}}/2$ contiguous beams within the beamset at each side.

Table 2
Parameters used for the simulation.

Parameter		Value
Transmission power	P_{tx}	[0, 23] dBm
Channel model		3GPP 37.885 [26]
Number of panels		4
Combined RF ports	N_{RF}	1 (fine), 3 (coarse)
Antennas per panel	N_{ant}	4
DFT Oversampling	O	1
Fine beams per panel	N_f	5
Coarse beams per panel	N_c	1
Aggregated pattern flattening	w_o	5.75
Simulation time		120 s
Central frequency	f	28 GHz
Bandwidth	BW	50, 100, 200 MHz
Subchannel size	N_{PRB}^{sch}	10 PRB
Number of neighbors	N_{ngh}	4, 6, 8, 10
Number of CSI bursts	K_{CSI}	1, 3

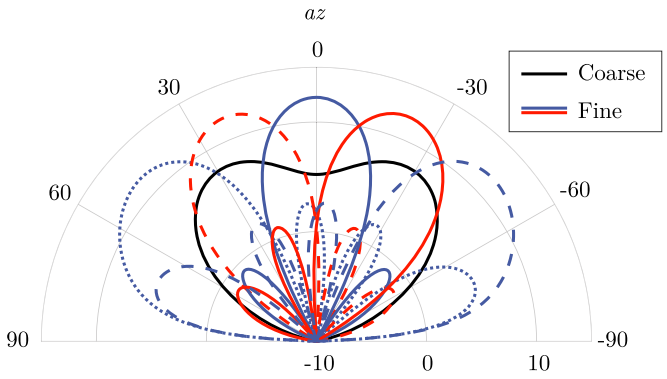

Fig. 4. Radiation pattern for the beamset used in the evaluation. Directivity [dB].

5. Results

The proposed strategies have been evaluated in terms of power performance and channel usage. In Table 2 the configuration parameters used for the simulation are detailed.

5.1. Power performance

The performance of both strategies has been measured for different configuration parameters. The power profile for each pair of nodes is compared with the reference beam alignment strategy in order to evaluate the overall performance of the proposed strategies. A two-level hierarchical beamset is built using $N_{ant} = 4$ antenna elements per panel, using 1 port for the fine beams and 3 ports for the coarse beams. The resulting pre-configured beamset for one panel, which is replicated and rotated to face the sector of each corresponding panel, is shown in Fig. 4. The resulting beams have a directivity of 12 dB and 7.9 dB for the fine and coarse configurations, respectively. The coarse beam has a half-power beamwidth of 94°, covering the whole sector, whereas the half-power beamwidth for the fine beams ranges from 24° to 35°, being sharper in the broadside. The most steered beams in neighboring panels overlap so that the panel switching is less frequent when the steering angle is at the edge of the steering range. A total of five fine beams and one coarse beams result from the calculations in (1) and (2), thus accounting for a total of 20 fine beams and four coarse beams using all panels.

From this beamset the beam management strategies are evaluated using different number of neighbors ($N_{ngh} = \{4, 6, 8, 10\}$). In Fig. 5, the mean time it takes for each configuration to recover from a misalignment is illustrated for the Manhattan scenario, where both LOS and NLOS visibility conditions are given. This recovery time is extracted from the instant at which the power

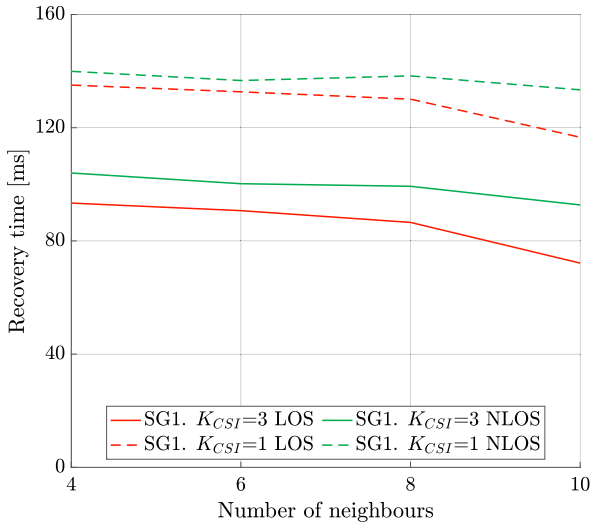

(a) Strategy 1.

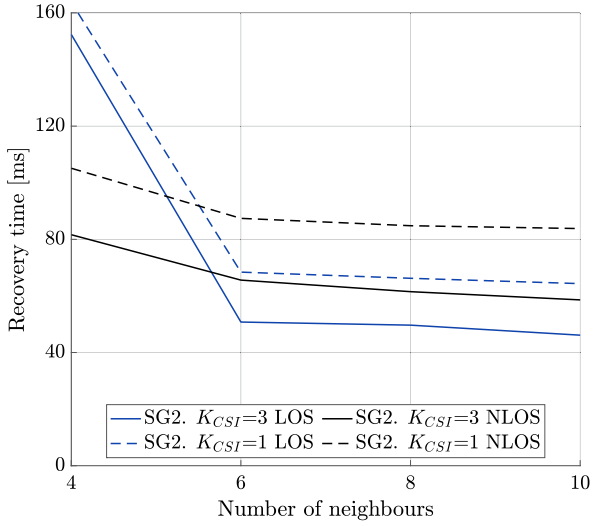

(b) Strategy 2.

Fig. 5. Mean recovery time of beam management strategies for different number of neighbors in LOS and NLOS visibility conditions.

profile deviates from the reference and ends when the strategy finds the same beam as the reference. Here, two values for K_{CSI} are considered. As CSI-based beam trainings occur in-between SSB burst, the K_{CSI} values being compared, 1 and 3, can be translated to a mean beam update rate of 80 ms and 40 ms, respectively. As seen in Fig. 5, the dashed lines correspond to a slower update and thus an increase in the mean recovery rate is shown in every situation. Strategy 2, in Fig. 5b, exhibits higher resilience to misalignment, as an increase in update rate only delivers a mean of 15.9 ms less recovery time in LOS conditions and 23.4 ms in NLOS conditions. Conversely, Strategy 1 (Fig. 5a) sees its recovery time improved from 38 ms to 42.9 ms when switching to a more frequent beam update rate, around twice the time compared to SG1. It is worth noting that none of the strategies gets severely impaired in terms of beam recovery when visibility conditions worsen, and NLOS conditions remain comparable to LOS in all cases.

From Fig. 5 it can also be seen how none of the configurations exceed 160 ms of sustained misalignment. This might appear obvious for SG1, as a full coarse beam search is performed every 160 ms, but also gives merit to SG2, which has no mechanism

to ensure certainty about the fact that the chosen beam is the optimum one. As for the number of neighbors, none of the considered configurations gets close to a perfect beamalignment, so full misalignment prevention may require more aggressive strategies. Nevertheless, all configurations at least appear to stabilize with a less ambitious beamset size. SG1 shows little improvement when changing from 4 to 10 neighbors. SG2 presents nonetheless a noticeable improvement when more than 6 neighbors are used, and it presents in this situation the best performance in terms of beam recovery.

To properly evaluate the damage exerted over the link quality due to the misalignment, the loss in power with respect to the reference profile is calculated for both strategies. In Fig. 6, the loss dimension when the strategies' power profiles deviate from the reference is shown. To visualize this loss, the complementary cumulative distribution function (CCDF) of the experienced losses for all vehicles is deemed convenient to evaluate which potential losses each strategy would experience. In Fig. 6, a noteworthy difference between scenarios can be seen, which can be due to the variability of the required pointing angles. Links in a Manhattan scenario may experience a wider range of potential angles of arrival in the same data session, whereas links in a highway scenario require less frequent beam switch. This increased beam update requirement in the Manhattan scenario, when handled by practical beam update rates and manageable beamsets, provides an increase in losses, as in some manoeuvres the optimum beam quickly deviates from the one being used.

In these results, 70% of the time the loss stays below 3 dB which, according to the ripple in the aggregated fine pattern, can be seen as if the chosen beam is generally the optimum one or one consecutive neighbor. Although this loss can be acceptable in normal operation, it is also important to consider the loss experienced at a low probability as it will eventually extrapolate to reliability at link level. When CCDF $= 10^{-1}$, the loss observed in Fig. 6 is exceeded 10% of the time. SG1 (Fig. 6a) presents then a 10% probability of exceeding a 10.9 dB power loss with $N_{\text{ngh}} = 4$ and 10.5 dB with $N_{\text{ngh}} = 10$ in the Manhattan scenario, and this margin when using different N_{ngh} slightly increases for the highway scenario – which ranges from 6.0 dB to 5.3 dB, respectively – consolidating further its independence from the number of neighbors. SG2 presents less power loss with the same probability, with 8.2 dB for the Manhattan scenario and 5.4 dB in highway for the case with 4 neighbors, a value that decreases uniformly around 1.5 dB when $N_{\text{ngh}} = 10$. Again, the increase in N_{ngh} makes a noticeable impact on SG2 (Fig. 6b) performance. It is also worth paying attention to the data when it approximates the 1% threshold. For the highway scenario – allegedly the best performing one – switching from 10 to 4 neighbors increases the 1% probability-conditioned loss more than 10 dB for SG1 and around 6 dB for SG2, and the losses quickly reach over 30 dB for the Manhattan scenario; a marginally-occurring but decisive loss that can severely impair the link down to outage and might be critical when aiming for negligible error rates.

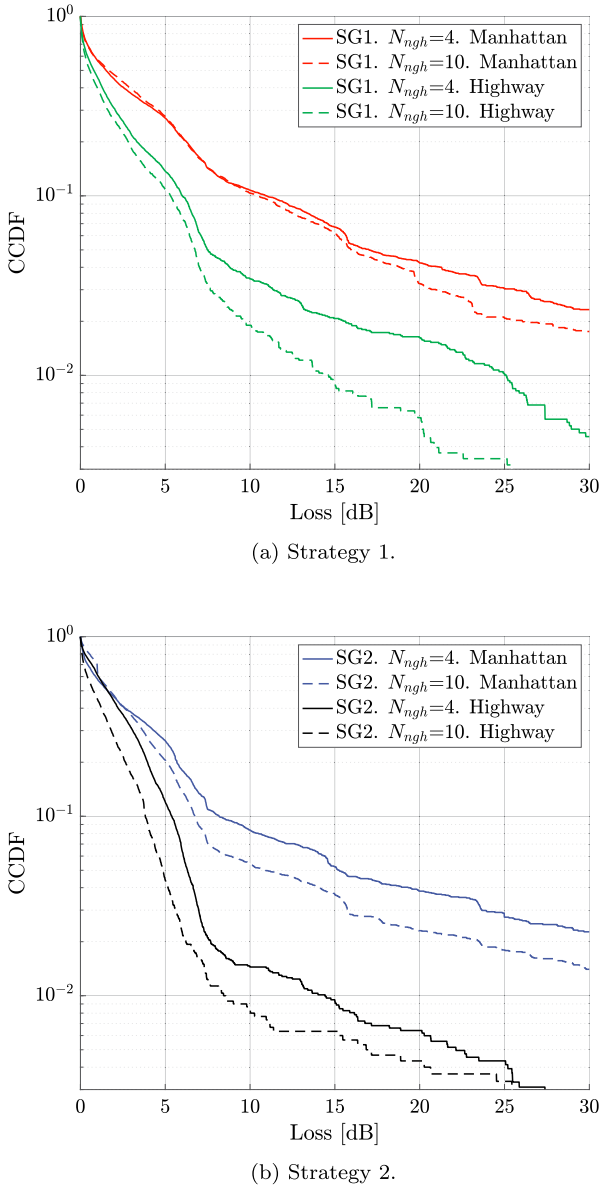

Fig. 6. Loss complementary cumulative distribution of beam management strategies in different traffic scenario for $N_{\text{ngh}} = \{4, 10\}$ and LOS conditions.

5.2. Channel usage

One relevant difference between the proposed strategies is the need for resources. SG1 is able to measure fine beams against a coarse anchor beam previously established, every CSI burst consists of $1 + N_{\text{ngh}}$ measurements and thus $2 \times (1 + N_{\text{ngh}})$ CSI resources are required to obtain a fine beam pair. Conversely, by using SS bursts also for fine beam tracking, SG2 needs to attempt all fine combinations every measurement, requiring $(1 + N_{\text{ngh}})^2$ CSI resources and therefore having exponentially increasing resource needs.

To measure the resource usage of each strategy, the interference sensed by receiving vehicles is calculated in a scenario where all vehicles are performing the same strategy. The traffic model in the highway scenario has been slightly modified to showcase an extreme case with very high vehicle density, in a way that all vehicles are separated with a safety time gap of 2.5 s [8]. The parameter used to compare resource usage is the Beam-based Channel Usage Ratio (BB-CUR), which represents the extent to which the channel is utilized by the occupied resources conditioned to the receiving beam in each case. Each link pair exchanges data with medium traffic intensity, which according to [26] implies a 20% and 80% chance of generating a 1.2 kbyte and 0.8 kbyte payload, respectively, with a 30 ms inter-packet reception rate; and also exchange the S-SSB and CSI resources required to align their beams. BB-CUR is thus calculated, for a 100 ms window, by measuring PRB-wise the intended data exchange and the sensed interferences captured by the receiving beam for each vehicle, and then averaging the sensed channel usage for all the vehicles with respect to the total resource pool capacity.

The share of the channel used when all the vehicles exchange data with the proposed strategies is shown in Fig. 7. Here, the BB-

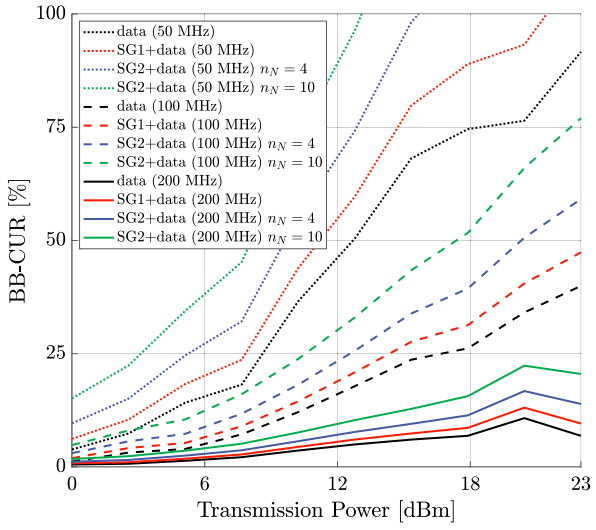

Fig. 7. Beam-based Channel Usage Ratio (BB-CUR) for medium intensity data traffic and the resources needed by the proposed strategies, compared for different total channel bandwidths (BW) and number of neighbors (N_{ngh}).

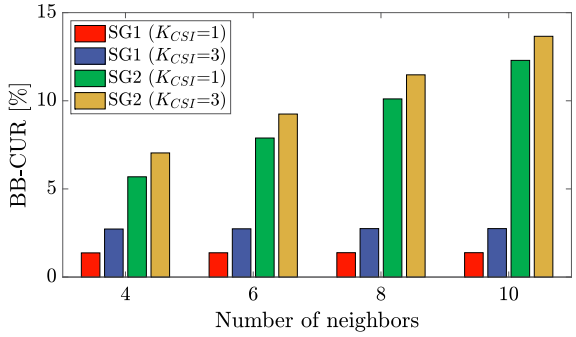

Fig. 8. Beam-based Channel Usage Ratio (BB-CUR) of the resources needed by the proposed strategies for different K_{CSI}, transmission power of 23 dBm and 200 MHz bandwidth.

CUR occupied by the data traffic with and without the overheads associated with each strategy is presented for different channel bandwidth options ($BW = \{50, 100, 200\}$ MHz) and transmission power (P_{tx}). The power transmitted, which is homogenized across the entire simulation for simplicity, affects the extent to which each radiated signal spans in space and therefore increases the coverage of an interfering wave. BB-CUR appears to increase linearly with the configured transmission power, yet at different rates depending on the total channel bandwidth. Indeed, our BB-CUR results for only data can be fairly approximated by BB-CUR [%] $\simeq 9.5\, P_{\text{tx}}\,[\text{dBm}]\, e^{-0.02\, BW\,[\text{MHz}]}$. The usage ratio when the strategies are used together with data increases considerably, and especially in the 50 MHz case none of the strategies would support the largest configurable P_{tx} [26] without exceeding the total pool capacity.

In these results, SG1 curves for different N_{ngh} are almost equal and an average of all N_{ngh} configurations is presented in Fig. 7. A data exchange using SG1 uses a smaller share of the channel compared to any of the evaluated SG2 configurations. Although how BB-CUR relates to the final link reliability is left out of the scope of this evaluation, some practical limits found in the literature can be applied to the study. According to [8], an usage ratio up to 80% might be reasonable for broadcast links with relaxed reliability requirements. However, for unicast/groupcast links where link reliability can be a stringent demand for some applications, the channel usage ratio must be significantly reduced. In this cited study, an usage ratio of 33.6% is used as an acceptable bound for reliable data exchange, based on results from [31]. Accordingly, such a threshold is easily surpassed in most of the evaluated cases, and the maximum power cannot be used for transmission. Only in the 200 MHz configuration, BB-CUR stays below 25% regardless of the strategy. However, for smaller channel bandwidths, the maximum P_{tx} that may be used in SG2 is from 2 dB to 4 dB lower to that of SG1, with the underlying loss in coverage for the same BB-CUR.

A closer look to the effects of the strategies on channel occupancy can be seen in the slice shown in Fig. 8. Here, the maximum transmission power is used ($P_{\text{tx}} = 23$ dBm) to exemplify the highest levels of BB-CUR. Channel usage is not significantly affected by the increase of CSI bursts, and BB-CUR increases less than 2 percentage points when the beam is more frequently updated. The number of neighbors does however affect SG2. While N_{ngh} makes negligible increments for SG1, the BB-CUR for SG2 increases linearly and is twice as high for 10 neighbors compared to 4. SG2 presents always the largest values of BB-CUR, even for 4 neighbors, where the channel usage is 4 times the one experienced in SG1 in the $K_{\text{CSI}} = 3$ case.

6. Conclusions

The use of multi-element antenna systems in vehicles stands as a promising enabler for the most demanding driving applications foreseen in the connected and automated future of transportation. The millimeter wave band and its large available bandwidths will be the next step to support the most data-hungry services, however the use of beamforming to target surrounding V2X nodes might is essential to overcome the propagation hurdles at these bands. Handling rapidly variant vehicular scenarios is nonetheless cumbersome when the beams between connected pairs need to be continuously aligned, and therefore a framework for beam management in vehicular scenarios should be considered to advance in the field.

In this paper the possibilities for beamformed vehicular communications with the currently specified NR-V2X mechanisms are described. With these considerations, two beam management strategies have been proposed, inspired by conventional procedures used today for links with the base station. The strategies are analyzed in terms of power performance – addressing time and power loss related issues – and channel usage, materialized here as the Beam-based Channel Usage Ratio (BB-CUR).

The proposed strategies differ fundamentally in the approach to maintain the optimum beam pair from a subset of beams, either by establishing a wide-beam anchor and refining (Strategy 1) or by constantly measuring a subset of sharp beams (Strategy 2). The latter appears to show reduced power loss and beam recovery time than its non-anchored counterpart with a relatively small beamset size; whereas both approaches see these metrics improved when beams are more frequently updated.

Although operating just with fine beams (Strategy 2) presents the best performing power metrics, Strategy 1 remains stable regardless of the beamset size, so having a coarse anchor beam appears to give predictable results unless this one deviates from the optimum. When the resource usage of each configuration is assessed, attempting to measure all beam combinations within a beamset quickly becomes unwieldy, and the channel occupancy of the required signaling outweighs the benefits in power performance obtained with this apparently more agile strategy. As resource-intensive configurations will become unfeasible for small channel bands, the stability and low usage here exhibited by the anchored strategy may turn into the only option when high reliability is pursued. As the results suggest, resource usage appears more dependent on the angular span of the beamset being used than on the measurement rate performed by the training pairs

The considerations, strategies and results presented in this paper aim to serve as an input for this open research field by focusing on realistic channel and antenna realizations. Further studies such as the analysis of the effects of the interference exerted by these beams on scheduling and the potential of these beamformed links to intensify the re-use of resources are left out of the scope of this document and left as a future work. By interpreting the results, the analysis of these or similar strategies with added layers of communications might elucidate the required information needed for fail-safe beam alignment, the potential new control messages that will need to be exchanged, and overall the required methodologies needed to eventually enable beamformed, autonomously managed vehicular communications that could support the required services in the autonomous vision.

Declaration of competing interest

The authors declare that they have no known competing financial interests or personal relationships that could have appeared to influence the work reported in this paper.

Acknowledgement

This work was partly funded by the Spanish Comisión Interministerial de Ciencia y Tecnología under projects TEC2013-47360-C3-1-P, TEC2016-78028-C3-1-P and MDM2016-0600, and Catalan Research Group 2017 SGR 219. The Spanish Ministry of Education (FPU17/05561) and Generalitat de Catalunya DI programme (2018-DI-084) also contribute with predoctoral grants for the authors.

References

[1] Huawei-HiSilicon, Sidelink synchronization mechanisms for NR V2X, Technical Document R1-1901539, 3rd Generation Partnership Project (3GPP), March 2019.
[2] Huawei-HiSilicon, Beamforming for V2X sidelink for FR1 and FR2, Technical Document R1-1903075, 3rd Generation Partnership Project (3GPP), March 2019.
[3] D. Medina, L. Hu, H. Rosier, S. Ayaz, Interference-aware dynamic resource allocation for D2D proximity services with beamforming support, in: 2015 IEEE Global Communications Conference, GLOBECOM, IEEE, 2015, pp. 1–7.
[4] Y. Feng, D. He, Y. Guan, Y. Huang, Y. Xu, Z. Chen, Beamwidth optimization for millimeter-wave V2V communication between neighbor vehicles in highway scenarios, IEEE Access 9 (2020) 4335–4350.
[5] 3GPP, Technical Specification Group Radio Access Network; Study on New Radio Access Technology; Physical Layer Aspects; (Release 14), Technical Report (TR) 38.802, 3rd Generation Partnership Project (3GPP), version 14.2.1, September 2017.
[6] 3GPP, Technical Specification Group Radio Access Network; NR; Physical channels and modulation; (Release 16), Technical Specification (TS) 38.211, 3rd Generation Partnership Project (3GPP), version 16.3.0, September 2020.
[7] 3GPP, Technical Specification Group Radio Access Network; NR; Radio Resource Control (RRC) protocol specification (Release 16), Technical Specification (TS) 38.331, 3rd Generation Partnership Project (3GPP), version 16.4.1, March 2021.
[8] 5GAA, Working Group Standards and Spectrum; Study of Spectrum Needs for Safety Related Intelligent Transportation Systems - Day 1 and Advanced Use Cases, Technical Report (TR) TR S 200137, 5G Automotive Association, version 1.0, June 2020.
[9] 3GPP, Technical Specification Group Radio Access Network; NR; Study on NR Vehicle-to-Everything (V2X); (Release 16), Technical Report (TR) 38.885, 3rd Generation Partnership Project (3GPP), version 16.0.0, March 2016.
[10] V. Petrov, J. Kokkoniemi, D. Moltchanov, J. Lehtomäki, M. Juntti, Y. Koucheryavy, The impact of interference from the side lanes on mmWave/THz band V2V communication systems with directional antennas, IEEE Trans. Veh. Technol. 67 (6) (2018) 5028–5041.
[11] O.A. Saraereh, A. Ali, I. Khan, K. Rabie, Interference analysis for vehicle-to-vehicle communications at 28 GHz, Electronics 9 (2) (2020) 262.
[12] C. Perfecto, J. Del Ser, M. Bennis, Millimeter-wave V2V communications: distributed association and beam alignment, IEEE J. Sel. Areas Commun. 35 (9) (2017) 2148–2162.
[13] V. Va, T. Shimizu, G. Bansal, R.W. Heath Jr., Millimeter wave vehicular communications: a survey, Found. Trends Netw. 10 (1) (2016) 1–118.
[14] B. Coll-Perales, J. Gozalvez, M. Gruteser, Sub-6GHz assisted MAC for millimeter wave vehicular communications, IEEE Commun. Mag. 57 (3) (2019) 125–131.
[15] T. Shimizu, V. Va, G. Bansal, R.W. Heath, Millimeter wave V2X communications: use cases and design considerations of beam management, in: 2018 Asia-Pacific Microwave Conference, APMC, IEEE, 2018, pp. 183–185.
[16] M. Brambilla, L. Combi, A. Matera, D. Tagliaferri, M. Nicoli, U. Spagnolini, Sensor-aided V2X beam tracking for connected automated driving: distributed architecture and processing algorithms, Sensors 20 (12) (2020) 3573.
[17] S. Akoum, A. Thornburg, X. Wang, A. Ghosh, Robust beam management for mobility in mmWave systems, in: 2018 52nd Asilomar Conference on Signals, Systems, and Computers, IEEE, 2018, pp. 1269–1273.
[18] V. Va, J. Choi, R.W. Heath, The impact of beamwidth on temporal channel variation in vehicular channels and its implications, IEEE Trans. Veh. Technol. 66 (6) (2016) 5014–5029.
[19] V. Va, R.W. Heath, Basic relationship between channel coherence time and beamwidth in vehicular channels, in: 2015 IEEE 82nd Vehicular Technology Conference, VTC2015-Fall, IEEE, 2015, pp. 1–5.
[20] S.-Y. Lien, D.-J. Deng, C.-C. Lin, H.-L. Tsai, T. Chen, C. Guo, S.-M. Cheng, 3PPP NR sidelink transmissions toward 5G V2X, IEEE Access 8 (2020) 35368–35382.
[21] Huawei-HiSilicon, Sidelink synchronization mechanisms for NR V2X, Technical Document R1-1901539, 3rd Generation Partnership Project (3GPP), November 2019.
[22] 3GPP, Technical Specification Group Radio Access Network; NR; User Equipment (UE) radio transmission and reception; Part 1: Range 1 Standalone; (Release 17), Technical Specification (TS) 38.101-1, 3rd Generation Partnership Project (3GPP), version 17.0.0, December 2020.
[23] CATT, Feature lead summary on AI 7.2.4.3 Sidelink synchronization mechanism, Technical Document R1-191xxxx, 3rd Generation Partnership Project (3GPP), November 2019.
[24] 3GPP, Overall description of Radio Access Network (RAN) aspects for Vehicle-to-everything (V2X) based on LTE and NR (3GPP TR 37.985 version 16.0.0 Release 16), Technical Report (TR) TR 137 985, European Telecommunications Standards Institute (ETSI), version 16.0.0, July 2020.
[25] 3GPP, Technical Specification Group Radio Access Network; NR; Physical Layer Procedures for Data; (Release 16), Technical Specification (TS) 38.214, 3rd Generation Partnership Project (3GPP), version 16.3.0, September 2020.
[26] 3GPP, Technical Specification Group Radio Access Network; Study on Evaluation Methodology of New Vehicle-to-Everything (V2X) Use Cases for LTE and NR; (Release 15), Technical Report (TR) 37.885, 3rd Generation Partnership Project (3GPP), version 15.3.0, June 2019.
[27] P.A. Lopez, M. Behrisch, L. Bieker-Walz, J. Erdmann, Y.-P. Flötteröd, R. Hilbrich, L. Lücken, J. Rummel, P. Wagner, E. Wießner, Microscopic traffic simulation using SUMO, in: The 21st IEEE International Conference on Intelligent Transportation Systems, IEEE, 2018, https://elib.dlr.de/124092/.
[28] S. Noh, M.D. Zoltowski, D.J. Love, Multi-resolution codebook and adaptive beamforming sequence design for millimeter wave beam alignment, IEEE Trans. Wirel. Commun. 16 (9) (2017) 5689–5701.
[29] S. Jaeckel, L. Raschkowski, K. Börner, L. Thiele, Quadriga: a 3-d multi-cell channel model with time evolution for enabling virtual field trials, IEEE Trans. Antennas Propag. 62 (6) (2014) 3242–3256.
[30] X. Yin, X. Cheng, Propagation Channel Characterization, Parameter Estimation, and Modeling for Wireless Communications, John Wiley & Sons, 2016.
[31] 3GPP, Technical Specification Group Radio Access Network; Study on LTE-based V2X Services; (Release 14), Technical Report (TR) 36.885, 3rd Generation Partnership Project (3GPP), version 14.0.0, June 2016.